Hindawi
Journal of Spectroscopy
Volume 2023, Article ID 7802548, 12 pages
https://doi.org/10.1155/2023/7802548

Research Article

A Study of the Electronic Absorption and Emission Spectra of DBDMA Dye: Solvent Effect, Energy Transfer, and Fluorescence Quenching

Sadeq M. Al-Hazmy,[1] **Jameelah Al-Harby**,[1] **Mohammed Hassan**,[2] **Sabri Messaoudi**,[1] **Ibrahim A. Alhagri**,[1,2] **and Ahmed N. Alhakimi**[1,2]

[1]*Department of Chemistry, College of Science, Qassim University, Buraidah 51452, Saudi Arabia*
[2]*Department of Chemistry, Faculty of Science, Ibb University, Ibb, Yemen*

Correspondence should be addressed to Mohammed Hassan; m-hassan@ibbuniv.edu.ye

Received 15 November 2022; Revised 10 May 2023; Accepted 24 May 2023; Published 2 June 2023

Academic Editor: Rizwan Hasan Khan

This study is aimed to shed light on the electronic absorption and emission spectra of DBDMA (2-(1-(difluoroboraneyl)-1,2-dihydroquinolin-2-yl)-2-(1-methylquinoxalin-2-ylidene) acetonitrile) in different solvents. Both types of spectra were obtained theoretically and produced experimentally in different solvents. The photostability of dye was tested, and its energy transfer behavior in the presence of oxygen and hydrated copper sulfate quenchers was investigated. We also gave a qualitative estimation of the effect of acidic media on the absorption and emission spectra. There is good compatibility between the calculated and measured values of many photophysical parameters. DBDMA has a low chemical quantum yield in solvents of different polarities, and the fluorescence quantum yield is high enough, which confirms, together with the low values of the excited state lifetime, its efficiency as laser emitting dye in the range of wavelength emission maxima. The rigidity of the DBDMA molecule is the main reason for the photochemical stability and the absence of a considerable shift as a result of the change in the polarity of the solvents. Geometries of ground and excited states were optimized using the density functional theory (DFT) and the time-dependent density functional theory (TD-DFT), respectively. Upon using the TD-DFT method, the UV-Vis absorption and emission spectra of the DBDMA molecule in different solvents were illustrated. A slight change is observed in the position of the maximum emission and absorption wavelength with the change of the solvent due to the rigidity of the compound. There was no apparent effect of quenching by oxygen. Besides, no intersystem crossing (ISC) was observed for the excited state of the DBDMA as a result of aeration of a solution with O_2 for 20 min, which was an explanation of the stability of peak emission intensity of dye after exposure to oxygen gas. The energy transfer rate constant has been calculated as well.

1. Introduction

Boron dipyrromethene (BODIPY) complexes have drawn great attention in the last two decades because they are promising for applications in molecular probes [1], photodynamic therapy [2], laser dyes [3], nonlinear optical materials [4], and solar cells [5–7]. These applications are primarily based on their interesting photophysical properties, such as high chemical stability, high photoluminescence quantum yield, ground-state solid absorption, and intense fluorescent emission. In the past decade, the core structure of BODIPY has been adjusted and developed into its aza-derivatives, such as aza-boron dipyrromethene, aza-boron-diindolmethene, aza-boron-dipyridomethene, and aza-boron-diquinomethene [7, 8]. These compounds show good electron-transporting properties, enhanced photoluminescence quantum yields, and unusual thermal stability that can be exploited in organic light-emitting devices (OLEDs) [9–11]. Sathyamoorthi et al. synthesized pyridoamine-based BODIPYs for the first time in 1993 [12], and then Bañuelos et al. discovered their photophysical properties by 2011 [13]. Several quinoline-based complexes

showed better electron mobility than pyrrole and pyridine counterparts [14], indicating that the quinoline structure is also a promising candidate for constructing boron-fluorine complexes. Lately, an aza-boron-diquinomethene complex was reported by Kondakova et al. which was exploited as a deep blue fluorescent emitting material to fabricate white OLEDs [15]. Despite the obtained promising results, the investigation of the aza-boron-diquinomethene is still lagging. To improve the optical properties through structural modification, investigation of the structure-property relationship is critically important.

Both static and dynamic fluorescence quenching originate from fluorophore interactions with another molecule in its surrounding environment. It is well known that the solvent effects play a significant role in photochemical reactions and energy transfer processes in the solution system of BODIPY compounds. The type and extent of interaction between the solute and the solvent depend on the polarity of the solvent and the possibility of the formation of hydrogen bonds with the solute [16]. Besides, the influence of the solvent on the electronic absorption and emission spectra has been the subject of interest and was considered as a method to calculate the dipole moment of the solute in the excited state.

In this work, an attempt was devoted to investigating the photophysical properties of one of the diflouroboron BODIPY complexes, namely 2-(1-(difluoroboraneyl)-1,2-dihydroquinolin-2-yl)-2-(1-methylquinoxalin-2-ylidene) acetonitrile (DBDMA). DBDMA has been reported as a potential indicator for low γ-ray doses [17]. The absorption and fluorescence properties of the dye in sol-gel glass matrices were investigated and found that the photosol-gel glass matrix of the immobilized dye is the best compared to other different photosol-gel and organic-inorganic matrices [18].

The structure of the DBDMA dyes is shown in Scheme 1. As can be seen in the structure, the molecule contains four nitrogen atoms of three types of hybridizations and hence is expected to exhibit interesting spectral properties. The absorption and emission spectra of the molecule have been calculated using the TD-DFT method and compared with the measured ones. The effect of the solvent on both absorption and emission spectra has been discussed in relation to the polarity of the solvents. Also, the photostability of the molecule and the influence of quenchers were investigated.

2. Experimental Setup

DBDMA was gifted by Professor Dr. Ewald Daltrozzo of Konstanz University, Germany, and used as supplied. Organic solvents (Fluka and Puriss) were of spectroscopic grade, and it was found free from impurities that could affect the absorption spectra or fluorescence within spectral ranges 250–600 nm. UV-Vis electronic absorption spectra were recorded using a Shimadzu UV-Vis 1650-PC spectrophotometer, where steady-state fluorescence spectra were presented employing a quartz cuvette of 1 cm path length; the emission was monitored at 90° geometry using

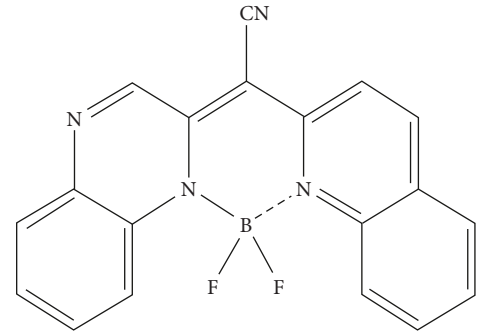

Scheme 1: The structure of DBDMA.

a Jasco FP-8200 spectrofluorometer with excitation bandwidth of 5 nm and emission bandwidth of 5 nm, using Xenon Lamp light source of 5 nm excitation and emission bandwidth.

Photochemical quantum yields of DBDMA (ϕ_c) were measured using a modified A. J. Lee's method that takes into consideration the decrease in absorbance at the excitation wavelength as photo-irradiation proceeds. The following equation (1) was applied to calculate the photochemical quantum yields:

$$\frac{dc}{dt} = \frac{-\phi_C \mathrm{I}_\circ \left(1 - 10^{-D}\right) \varepsilon b C}{D}, \tag{1}$$

where c is the concentration of DBDMA, t is the time in min, ϕ_c is the photochemical quantum yield, I_0 is the intensity of excitation light, D is the absorbance at the irradiation wavelength, ε is the extinction coefficient at irradiation wavelength, and b is the path length of the cell [19].

Typically, the samples were irradiated in a photoreactor equipped with a 400 W UV lamp set to 254 nm with a 250 microwatts/cm^2 irradiation intensity in an air atmosphere at ambient temperature.

Fluorescence quantum yields in liquid were estimated using the optically dilute solution relative method with either 9,10-diphenyl-anthracene or quinine sulfate solutions, depending on the emission wavelength range. The intensity of light was determined using ferrioxalate actinometry [20, 21]. The following equation (2) was applied to calculate the fluorescence quantum yields:

$$\varnothing_f(s) = \varnothing_f(r) x \frac{\int I_s}{\int I_s} x \frac{A_r}{A_s} x \frac{n_s^2}{n_r^2}. \tag{2}$$

The integrals refer to the corrected fluorescence peak areas, A is the absorbance at the excitation wavelength, and n is the solvent's refractive index. The subscripts s and r refer to the sample and reference, respectively.

The picosecond fluorescence decay patterns of DBDMA were determined by a picosecond pulse of (470 ± 10 nm) single-photon counting method using the FluoTime 300 (PicoQuant, Germany) in conjunction with the LDH-P-C-470 laser head. The equipment's lifetimes were determined using the FluoFit software. A Peltier-cooled photomultiplier (PMT) was utilized to detect photons emitted in the 300–900 nm region.

2.1. DFT Computational Study. Density functional theory (DFT) simulations using Gaussian 09 are used to optimize the chemical structures under study. In this work, the hybrid B3LYP functional is used [22]. It uses the 6-31G basis set and yields precise results. The optical characteristics of the investigated molecular structures are examined using the time-dependent DFT computations for the first twenty excited states. The used model for the solvent in this part is the PCM model.

The interaction between DBDMA and Cu^{+2} during dye fluorescence quenching with $CuSO_4.5H_2O$ was optimized through PBE1PBE functional and 6-31G (d)/Lanl2dz basis sets. For Cu, we applied the LANL2DZ basis set, and the calculations of all other atoms were performed by the 6-31G(d) basis set. TDDFT calculations combined with the solvation model SMD and ethanol were applied on the PBE1PBE optimized geometries with the PBEPBE1PBE/Lanl2DZ/6-31+G(d) level of theory [23] and were compared to the ligand at the same level of theory.

3. Results and Discussion

The spectroscopic and photophysical characteristics, solvent relative polarity, absorption, emission, and excitation maximum wavelengths, together with fluorescence and photochemical quantum yields of DBDMA in different solvents, are summarized in Table 1. Solvents were selected based on their ability to dissolve DBDMA and the difference in polarity and relative viscosity.

Figures 1S and 2S show the measured UV-visible absorption and emission spectra of DBDMA obtained at room temperature for a concentration of 1.4×10^{-5} mol·dm^{-3} in solvents of different polarities. The increase in solvent polarity slightly influences the position of electronic absorption and emission maxima. The blue shifts (hypsochromic shifts) in the absorption and emission maxima with increasing polarity of the medium indicate a decrease in the ground-state dipole moment of the dye molecule upon excitation with a concomitant increase in its ground-state dipole moment as a result of solvent polarization [24].

The experimental absorption spectra show narrow absorption bands with three absorption maxima similar in shape to boron dipyrromethene dyes [25]; for example, in CH_3CN, the band of a strong S_0–S_1 transition with a maximum at 508 nm, the shorter wavelength centered at about 478 nm together with that at 449 nm. Effect on the absorption maxima wavelength position was observed, where a shift in the direction of a shorter wavelength of around 10 nm is noticed by changing the solvent from ethanol, toluene, and THF at 521, 514, and 512 nm, respectively ($S_0 \longrightarrow S_1$ transition) to 508 nm in acetonitrile, as shown in Table 1 and Figure 1S. Figures 1 and 2 for the investigated dye demonstrate a strongly allowed $1(\pi\text{-}\pi*)$ transition with a small geometry change between electronic ground and excited states. This transition is consistent with the dye's high molar absorptivity and the mirror image relationship between excitation and fluorescence spectra in methylene chloride and carbon tetrachloride, respectively [26]. This is not the same as for the dye in butanol, as shown in Figure 3S, which shows a change in the geometry of the dye molecule when the photons were absorbed, as indicated by the disappearance of a mirror image relationship between the fluorescence spectra and electronic absorption.

The ability of butanol to make efficient hydrogen bonds with DBDMA might cause the relative loss of structured absorption and emission bands.

A more resolved Frank–Condon fluorescence peak is obtained at 560 nm. This transition appears as a shoulder with butanol and DMSO solvents. The small size and high polarity of acetonitrile lead to better solvation of excited BDBMA molecules with subsequent deactivation to a similar ground-state configuration [27]. The high purity of DBDMA is indicated by the coincidence between the absorption and excitation spectra in DMSO solvents, as shown in Figure 4S. Purity is also confirmed by the congruence between the two emission spectra of the dye using three different excitation wavelengths (Figure 5S). This congruence also indicates the absence of tautomers [28].

The Frank–Codon peak of the 0-0 transition in both fluorescence and absorption spectra occurs due to molecular rigidity. The very high polarity in the ground state due to the presence of fluorine and cyano-groups allows its rapid solvation, leading to a less vibrational resolution in the fluorescence spectra compared to the absorption spectra of DBDMA [29].

A minor Stokes shift of 8 nm is observed for the studied dye in the CCl_4 solvent, showing weak solvation in the excited state as illustrated in Figure 2. Besides, the emission spectrum shows a vibrational structure due to a lack of ground-state solvation. In ethanol, the lack of the vibrational structure of emission spectra in various solvents indicates higher ground-state solvation and the possibility of hydrogen bond formation that results in different excited state geometry from that of the ground state.

It is observed that there is an increase in Stokes shift with an increase in solvent relative polarity (Figure 3), indicating the increase in the dipole moment on excitation [30]. The resonance structures can explain the observed variations in the dipole moments. Indeed, DBDMA has been found to have a greater excited state dipole moment (μ_e) than that of the ground state (μ_g) [18].

3.1. Molecular Modeling and Quantum Chemical Parameters. The frontier molecular orbital (highest occupied molecular orbital (HOMO) and lowest unoccupied molecular orbital (LUMO)) of DBDMA was studied by using the B3LYB/6-31G level of theory as shown in Figure 4. π-bonding orbitals characterize the HOMO, and the LUMO is characterized by π^*anti-bonding orbitals. In the HOMO energy level (Figure 4), the π-bonding orbitals and lone pairs of electrons for all nitrogen atoms and two fluorine atoms are delocalized over the whole DBDMA molecule. Whereas in the LUMO energy level, the π^*anti-bonding orbitals and lone pairs of electrons for three nitrogen atoms are distributed over the whole probe dye, while the lone pairs of electrons for nitrogen atom in the cyanide (-CN) group and two fluoride

Table 1: Measured maximum absorption (λ_{abs}) and emission wavelengths (λ_{ems}) for the DBDMA molecule in different solvents.

Solvent	ETOH	Acetone	DMSO	ButOH	$CHCl_3$	CCl_4	CH_2Cl_2	DMF	CH_3CN	$CHBr_3$	THF
λ_{abs} max (nm)	521	510	511	511	512	517	513	512	508	519	513
λ_{em} max (nm)	540	527	533	535	532	525	523	530	523	532	612
E M^{-1} cm^{-1}	231034	3514	158620	120689	49655	22222	19493	200000	203448	8181	—
Relative polarity (Δf)	0.654	0.355	0.444	0.586	0.259	0.052	0.309	0.386	0.460	—	0.21
Stokes shift (cm^{-1})	19	17	22	24	20	8	10	18	15	—	—

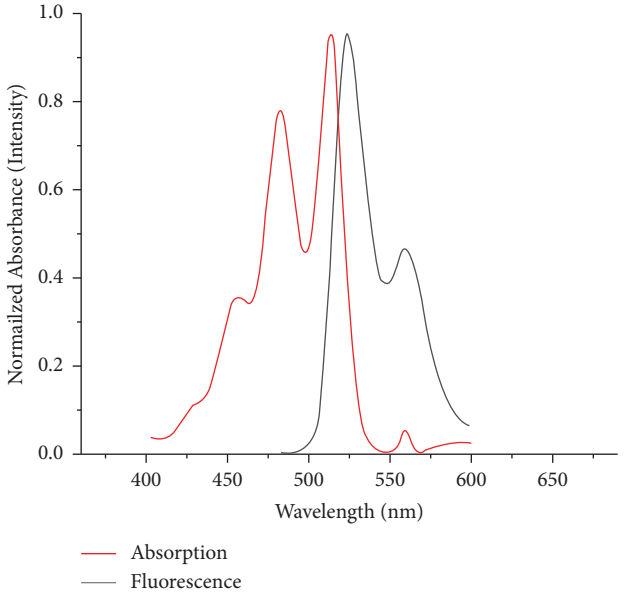

Figure 1: Normalized absorption and fluorescence spectra of 2.8×10^{-7} mol·dm^{-3} in CH_2Cl_2, $\lambda_{ex} = 512$ nm.

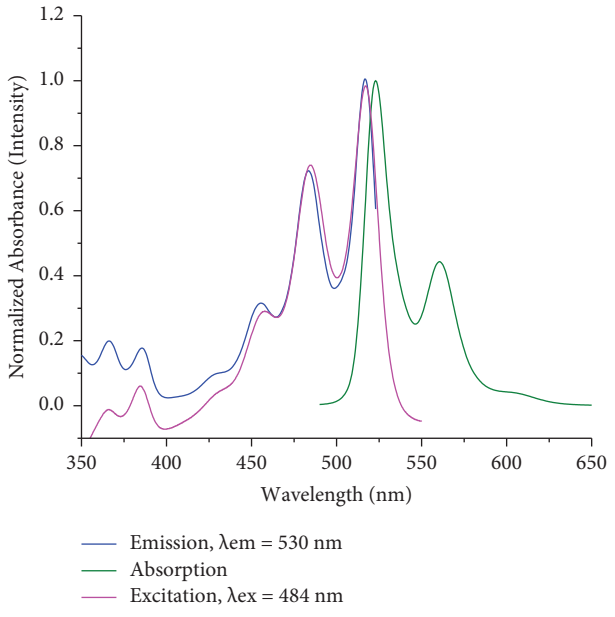

Figure 2: Normalized absorption, emission, and excitation spectra of 1.4×10^{-5} mol·dm^{-3} DBDMA in CCl_4.

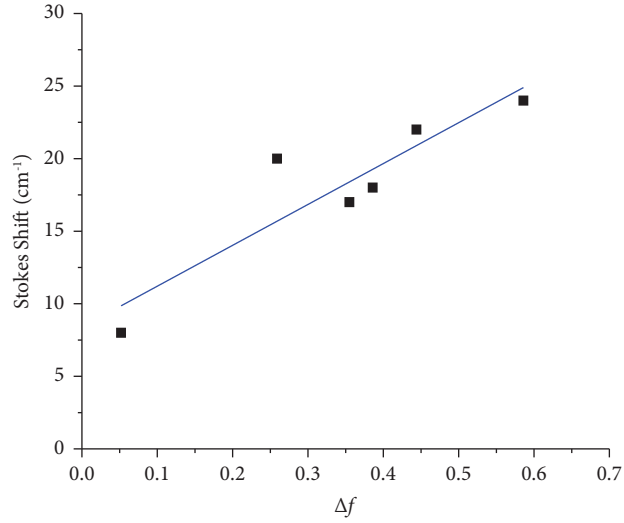

Figure 3: The variation of Stokes shift with the relative polarity of the solvents.

atoms do not take part in the distribution over the whole molecule.

Upon using the orbital energy level at the B3LYB/6-31G level of theory, the effect of different solvents on HOMO and LUMO energy orbitals, HOMO-LUMO energy gap (E_g), zero-point energy (ZPE), and dipole moment (μ) are produced and given in Table 2. When the magnitude of (E_g) increases, the kinetic stability of the molecule increases, and chemical reactivity decreases. Hence, the kinetic stability of the DBDMA molecule in dimethyl sulfoxide (DMSO) is the highest (Table 1) compared to other solvents due to the higher polarity of DMSO. As shown in Table 1, the value of E_g for the titled molecule increases with increasing the solvent polarity indicating a blue shift in absorption spectra for probe dye. The value of zero-point energy (ZPE) for DBDMA is decreased upon increasing solvent polarity, as shown in Table 2, indicating the high stability of the titled molecule in DMSO compared to other solvents. The increased dipole moment reveals large intramolecular charge transfer (ICT) in the molecule. Hence, the ICT for probe dye in DMSO is highest compared to other solvents.

Using the B3LYB/6-31G level of theory and the DFT method, the optimized structure for DBDMA is obtained and presented in Figure 5(b). Also, the charge distribution of each atom and the direction of dipole moment in the

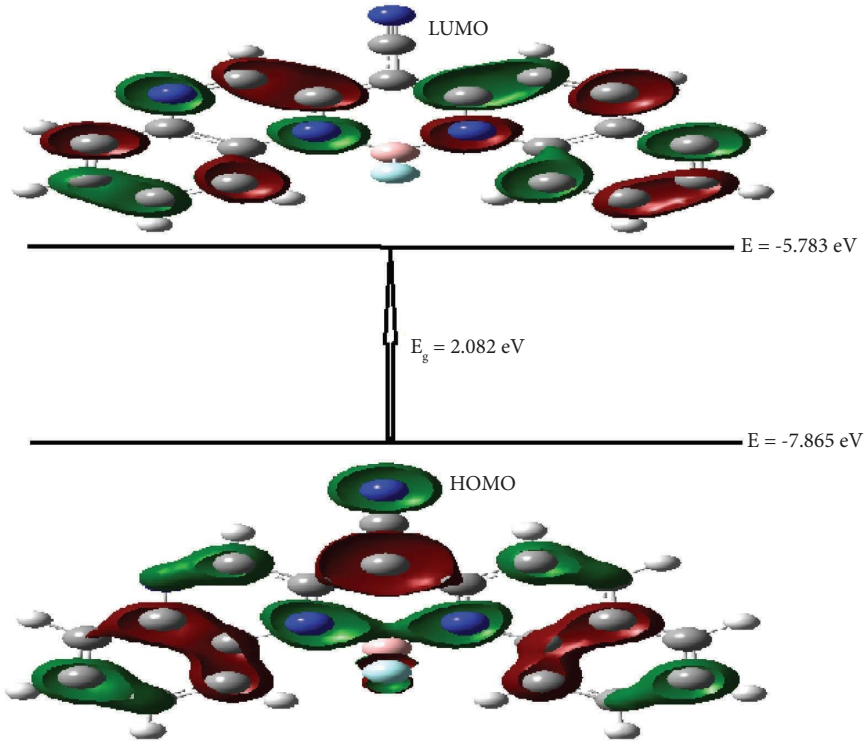

Figure 4: The graphical presentation of the highest occupied molecular orbital (HOMO) and lowest unoccupied molecular orbital (LUMO) of DBDMA dye in gas at the B3LYB/6-31G level of theory.

Table 2: The effect of solvent's polarity on HOMO energy, LUMO energy, HOMO-LUMO energy gap (E_g), zero-point energy (ZPE), and dipole moment (μ) of DBDMA.

Solvents	Polarity	E_{HOMO} (eV)	E_{LUMO} (eV)	E_g (eV)	ZPE (eV)	μ (D)
Gas	—	−7.865	−5.783	2.082	−31948.714	4.44
Carbon tetrachloride	0.052	−5.920	−2.843	3.077	−31948.904	5.05
Methylene chloride	0.259	−5.939	−2.847	3.092	−31834.710	5.56
Chloroform	0.309	−5.933	−2.840	3.093	−31949.013	5.40
Acetone	0.355	−5.945	−2.850	3.095	−31949.122	5.67
Dimethyl sulfoxide	0.444	−5.947	−2.852	3.096	−31949.130	5.67

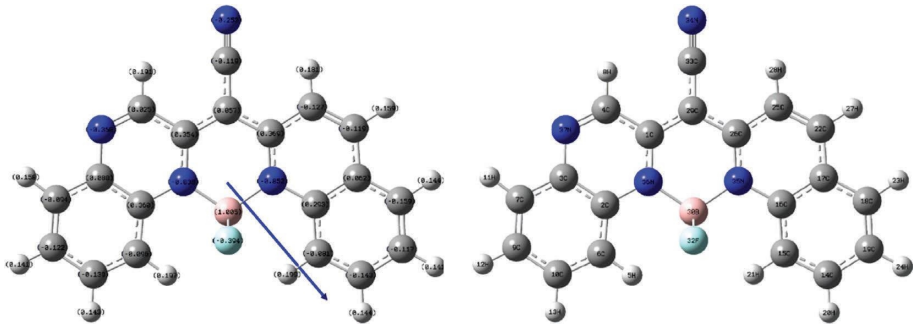

(a) (b)

Figure 5: The optimized structure for probe dye at the B3LYB/6-31G level of theory (b) and the charge distribution and the direction of dipole moments (a).

optimized structure are illustrated in Figure 5(a). From the DBDMA optimized structure, boron (30B) and nitrogen (35N) atoms have the highest positive (+1.005) and negative (−0.852) charges, respectively.

The calculated HOMO-LUMO gap for most of the selected solvents shows values between 3.092 and 3.093 except for CCl_4 which shows a smaller value of 3.077 and thus a higher wavelength. This is in agreement with experimental results which show that $\lambda_{\text{abs max}}$ for the selected solvents are between 510 and 513 nm except for CCl_4 which is 517 nm. The higher HOMO energy value when the molecule is surrounded by CCl_4 contributes to this smaller energy gap.

3.2. Effect of the Solvent on the Absorption and Emission Spectra. The UV-Vis absorption and emission spectra for the DBDMA molecule in different solvents such as CCl_4, CH_3Cl, CH_2Cl_2, acetone, and DMSO upon using the TD-DFT method were obtained and are illustrated in Figures 6(a) and 6(b). According to the molecular orbital theory (MOT), the allowed electronic transitions for the DBDMA molecule are $\sigma - \sigma^*$, $\pi - \pi^*$, $n - \sigma^*$, and $n - \pi^*$. For the DBDMA molecule in the gas phase, the UV-Vis absorption spectra showed two maximum absorption wavelengths at 291 and 448 nm. The maximum absorption wavelength for probe dye at 291 nm disappeared in polar and nonpolar solvents. Depending on the polarity of the solvent, the maximum absorption wavelength for DBDMA is shifted to longer wavelengths (red-shift) when the polarity of the solvents is decreased, as shown in Figure 6 and Table 3. The calculated spectra in Figure 6 simulate the intensities, which are based on the oscillator strength found in Table 3.

The emission spectra of DBDMA dye in different solvents show two bands of maximum emission wavelengths depending on the polarity of the solvents. Due to the high polarity of DMSO compared to other solvents and the gas phase, the λ_{max} emission for the titled molecule in DMSO is shifted to red (536 nm) compared to other solvents and the gas phase [31].

TD-DFT calculations show qualitative agreement with experimental results. First, it confirms what we have deduced from energy gaps that the molecule in CCl_4 has the highest absorption value. Second, it shows that the highest emission wavelength for the dye occurs in DMSO, which agrees with the experimental results. Among the selected solvents, DMSO has the highest polarity, and the TD-DFT calculations show that the DMSO solvent stabilizes the energy of the excited state to a much greater extent than the ground state and thus gives the highest emission wavelength.

3.3. Effect of Medium Acidity. No change in the absorption spectral pattern of DBDMA was observed due to the addition of acid, as shown in Figure 7. The vibronic peaks occur nearly at the same wavelengths, either in neutral, acidic, or basic media. The broadening in some peaks in basic media is probably due to more hydrogen bonding. It seems that the lone pair electron transition ($n - \pi$) plays a minor role in modifying electronic spectra compared with the ($\pi - \pi$) transitions. Also, Figure 7 shows that neither protonation nor deprotonation has happened in the ground state.

On the other hand, a slight red shift in the emission spectrum of DBDMA occurs upon the addition of sulfuric acid, as shown in Figure 8.

3.4. Photostability. The photochemical quantum yield (Φ_c) values (~0.003±) of DBDMA in four solvents are summarized in Table 4. The value of fluorescence quantum yield in ethanol surpassed that of BNTVB [32] and that of the dye itself when was impeded in a sol-gel matrix [18]. The low values of Φ_c indicate a photostability against irradiations, which is attributed to the rigidity of the molecules, which has also been confirmed by the small shifts in the emission and absorption wavelengths as the solvent's polarities change. The molecule's rigidity has also been indicated by the theoretical calculations, which produced a high fluorescence quantum yield. DBDMA dye has promising applications in many fields, including dye lasers and solar cell collectors, due to its apparent photochemical stability in low chemical quantum yield (Φ_f) and high fluorescence quantum yield.

DBDMA has short excited state lifetime values, as shown in Table 5. The short-excited state lifetime values indicate no influence of solvent polarity on the excited state duration. This short-excited state lifetime, together with high fluorescence quantum yield, confirms the ability of the dye to give laser emissions in the studied solvents. Fig. 6S shows the fluorescence decay profile of DBDMA in DMF, their exponential fit, and IRF. A quiet agreement between the time-resolved fluorescence curve and the fitted exponential data is observed, which indicates the applicability of the selected model. The plot of regular residuals (on the bottom of the curve confirms) confirms the successful application of the exponential model.

3.5. Quenching by Oxygen. Upon aeration of a solution of BDBMA in ethanol with O_2 for 20 mins, no effect on the photophysical deactivation pathway of BDBMA was observed for the excited state, which was an explanation of the stability of peak emission intensity of the dye after exposure to oxygen gas as shown in Figure 7S. This behavior is confirmed by measurement of the fluorescence quantum yield of the aerated solution of BDBMA, ϕ_f, which was found to be 0.83, confirming that molecular oxygen did not enhance the electronic transition from the singlet state to the excited triplet states through intersystem crossing (ISC) via its paramagnetic ground state. A prohibited singlet to triplet transition is crucial in laser media as the triplet population always has a deteriorating effect in laser media.

3.6. Energy Transfer. DBDMA is used as an energy acceptor from fluorescein dye. Low concentrations of the acceptor, which have low molar absorptivity at 459 nm, were used to avoid reabsorption. A mixture of DBDMA and fluorescein gave fluorescence emission spectra in the range 490 to 600 nm with an emission maximum of 530 nm upon excitation using λ_{ex} 459 nm light, as shown in Figure 9.

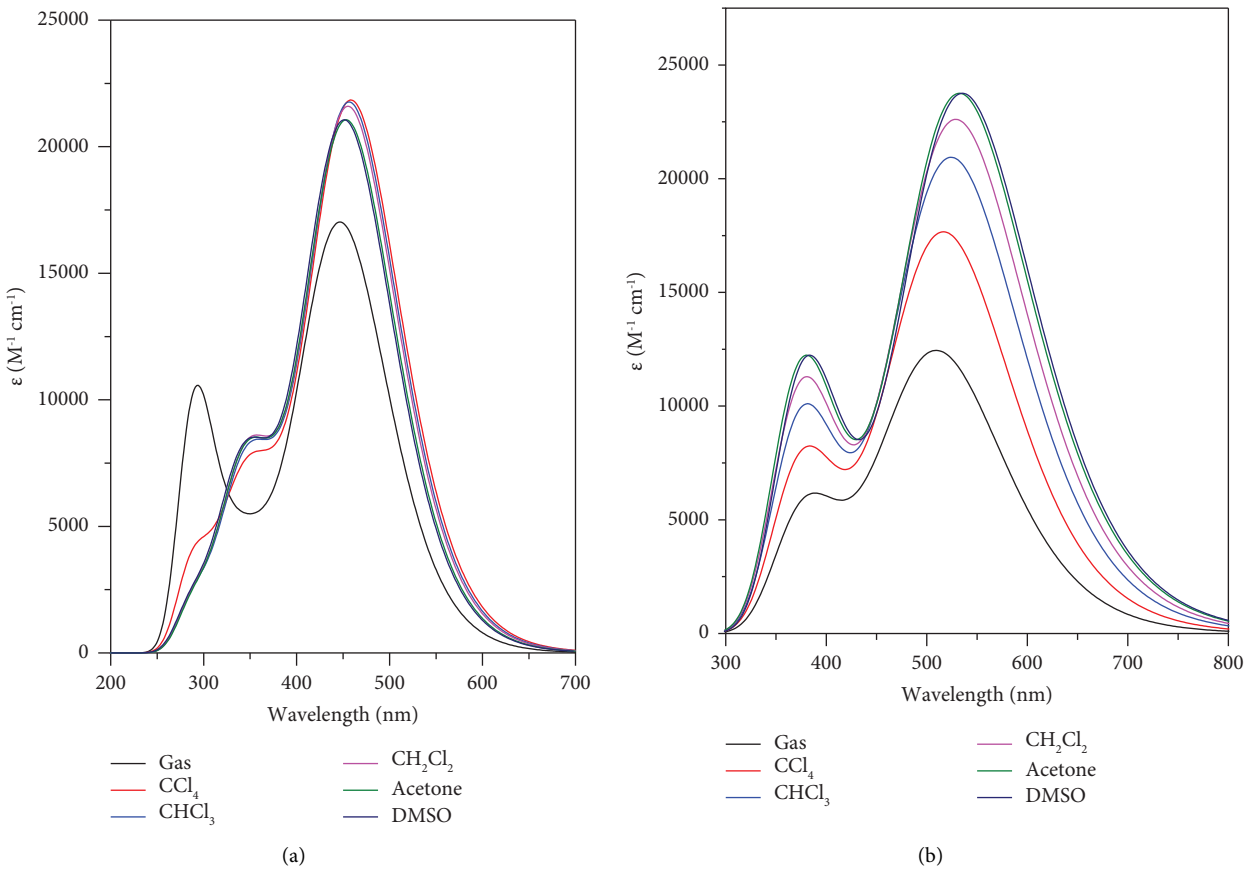

Figure 6: Calculated absorption (a) and emission (b) spectra for the DBDMA molecule in different solvents.

Table 3: Calculated maximum absorption (λ_{abs}) and emission wavelengths (λ_{ems}) for the DBDMA molecule in different solvents.

Solvent	Calculated using the TD-DFT method			Measured	
	$\lambda_{abs.}$ (nm)		$\lambda_{ems.(nm)}$	$\lambda_{abs.}$ (nm)	$\lambda_{ems\cdot(nm)}$
Gas	291	448	511	—	—
Carbon tetrachloride	—	460	517	517	525
Chloroform	—	458	525	512	532
Methylene chloride	—	457	529	513	523
Acetone	—	454	533	510	527
DMSO	—	452	536	511	533

The critical transfer distance R_o has been calculated for the fluorescein/DBDMAs energy transfer system by applying the relation:

$$R_o^6 = 1.25\,x\,10^{-25}\frac{\varnothing_D}{n^4}\int_0^{\infty} F_D(\overline{\nu})\epsilon_A(\overline{\nu})\frac{d\overline{\nu}}{\overline{\nu}^4}, \quad (3)$$

where R_o is the distance at which the energy transfer and emission processes are equally probable, ϕ_D is the emission quantum yield of the donor in the absence of the acceptor, n is the solvent refractive index, and the integral is the overlap integral for the fluorescence spectrum of donor normalized to unity (F_D) and the absorption spectrum of the acceptor ($\mathcal{E}_A$) divided by the fourth power of the wavenumber ($\overline{\nu}$).

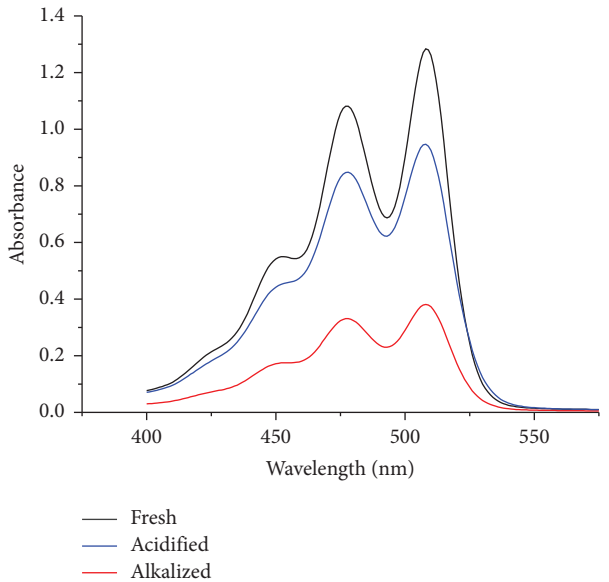

Figure 7: Absorption spectra of 1.41×10^{-5} mol·dm^{-3} of DBDMA in acetonitrile with different acidic media.

The significant difference in the value of the critical transfer distance R_o calculated from the donor-acceptor spectral overlap region (see Figure 10), 47 Å, is ~10 times greater than those characterizing collisional energy transfer,

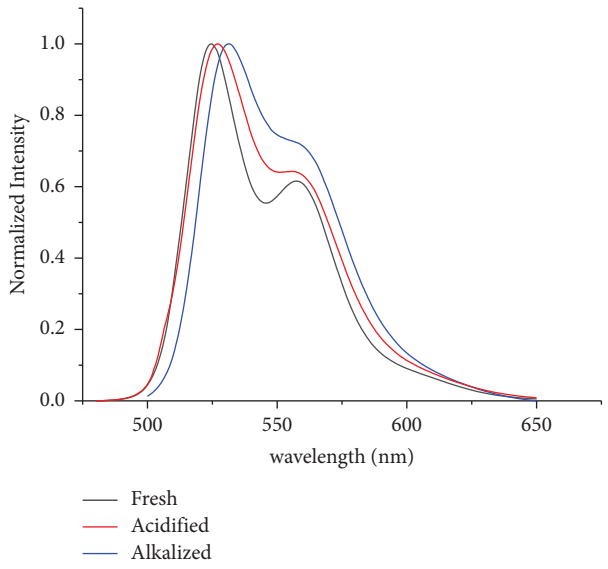

Figure 8: Fluorescence spectra of 1.4×10^{-5} mol·dm^{-3} of DBDMA in acetonitrile with different acidic media.

Table 4: Fluorescence quantum yield (ϕ_f), photochemical quantum yield (ϕ_c), and relative polarities of DBDMA in different solvents.

Solvent	ϕ_f		ϕc	Δf
	λ_{abs} max	λ_{ex} 449 nm		
EtOH	0.83		0.003	0.378
Acetone	0.41		—	0.355
DMSO	0.28		—	0.373
BuOH	0.1		0.003	0.358
DMF	0.34		0.004	0.390
CCl_4	0.68		0.005	0.052
Acetonitrile	0.79	0.31	0.003	0.386

Table 5: Excited state lifetime of DBDMA in different solvents at room temperature.

Solvent	τ (ns) ± 2%
Ethanol	4
Methanol	4.2
DMF	4.5
CH_3CN	3.9

for which R_o is in the range 4–6 Å, indicating that the underlying mechanism of energy transfer is that of resonance energy transfer due to long-range dipole-dipole interaction between the excited donor and the ground-state acceptor [33].

3.7. Quenching by $CuSO_4.5H_2O$. DBDMA has the advantages of a high extinction coefficient (11586 M^{-1}·cm^{-1}) at 514 nm and a strongly fluorescent dye with a high fluorescence quantum yield of 83% in ethanol at emission maxima around 530 nm. The addition of Cu^{2+} ions causes fluorescence quenching because of the heavy atom effect and the paramagnetic nature of Cu^{2+} ions. Successive addition of

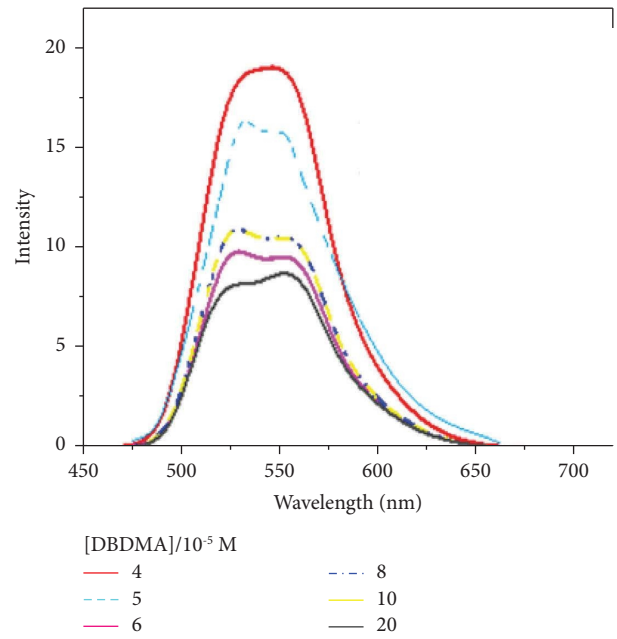

Figure 9: Fluorescence spectra of 1×10^{-2} M fluorescein at different quencher (DBDMA) concentrations (λ_{ex} 459 nm).

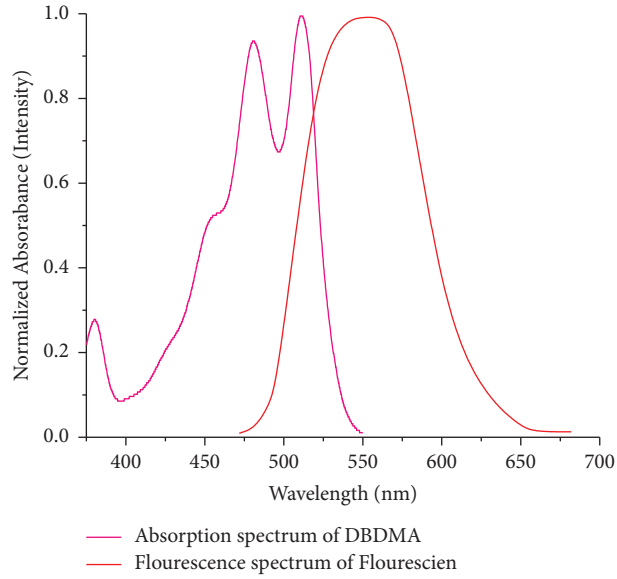

Figure 10: Overlap between the normalized absorption spectrum of 1.4×10^{-5} M DBDMA and the fluorescence spectrum of 1×10^{-2} M fluorescein in DMF.

Cu^{2+} in the form of copper sulfate pentahydrate results in a gradual decrease in the emission at the wavelength 530 nm as shown in Figure 11, accompanied by a slight bathochromic shift of ca. 3 nm in ethanol.

The Stern–Volmer plot of the quenching process of the dye using Cu^{+2} metal ion is shown in Figure 8S. A linear plot is obtained down to $CuSO_4.5H_2O$ concentration of 4×10^{-7} M, indicating an efficient quenching effect of Cu^{+2} ions [34].

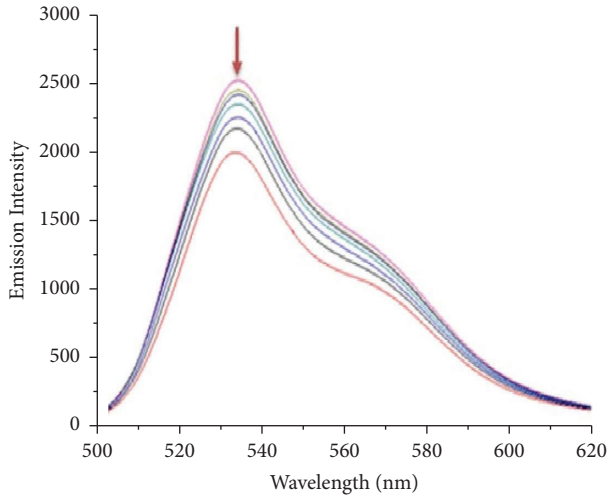

Figure 11: Fluorescence spectra of 1×10^{-5} mol dm^{-3} DBDMA in ethanol; increase in Cu^{2+} results in a decrease in emission intensity at 0.0, 4×10^{-7}, 1×10^{-6}, 4×10^{-6}, 6×10^{-6}, 8×10^{-6}, and 1.6×10^{-5} M $\lambda_{ex} = 512$ nm.

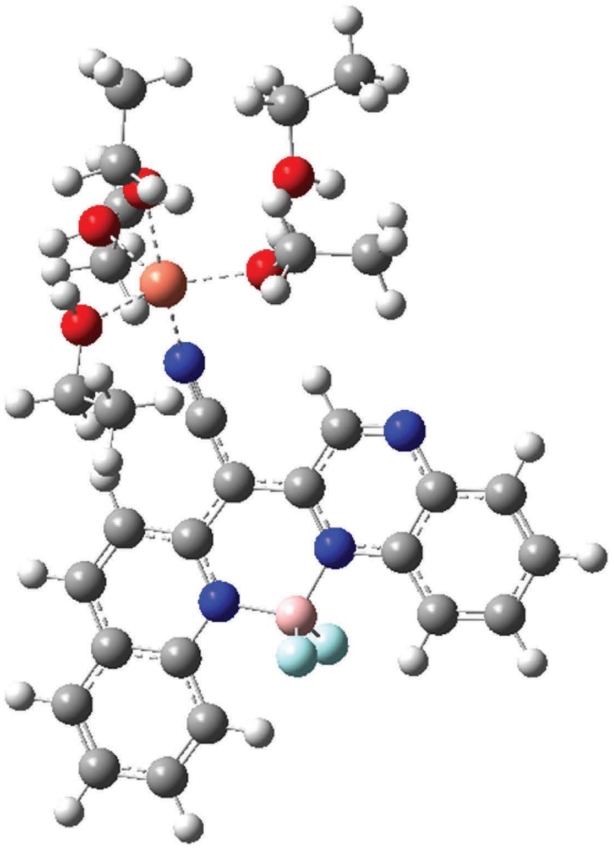

Figure 12: The DFT optimized structure of the Cu(II) complex model in the presence of ethanol molecules.

The rate constant (k_{ET}) of energy transfer in the DBDMA/fluorescein system in ethanol was calculated using the Stern–Volmer equation and the Stern–Volmer plot (Figure 8S). Excited state lifetime in DMF was measured as 4.5 ns. The Stern–Volmer relation in the following form was applied [35]:

Table 6: TDDFT results of selected electronic transitions, their absorption energies, and their oscillator strengths.

Complex	Transition	λ (nm)	Oscillator strength
Ligand	HOMO ⟶ LUMO	448	0.5583
Cu complex	HOMO(b) ⟶ LUMO(b)	746	0.0703

$$\frac{I_o}{I} = 1 + k_{ET}\tau[Q], \tag{4}$$

where I_o and I are fluorescence intensities in the absence and the presence of the quencher of concentration (Q), respectively, and τ is the e excited state lifetime of the donor in ethanol (4 ns). K_{ET} has been calculated as 3.70×10^7 M^{-1}·S^{-1}.

The optimized structure of the complex with Cu in the presence of ethanol molecules is shown in Figure 12. This study was conducted to compare the theoretical results to those obtained experimentally in ethanol.

The coordinates for the ligand and the Cu complex are found in the supplementary material (Tables 1S and 2S). The copper center is five coordinated and bonded to the ligand through one nitrogen atom. The bond length of Cu-N is 1.98 Å. Table 1 shows the TDDFT results of selected electronic transitions, their absorption energies, and their oscillator strengths. The electron density in the ligand alone is mainly located on the rings for the HOMO and the LUMO (Figure 13). In the Cu complex, the transition from the HOMO to LUMO shows an intramolecular charge transfer (ICT): in the HOMO, the electron density is mainly distributed on the rings, but in the LUMO it is mainly located on the metal (Figure 13). We may suggest that the ICT from ligand to metal leads the quenching of the fluorescence in this complex. The small value of the oscillator strength of this transition (Table 6) supports this result.

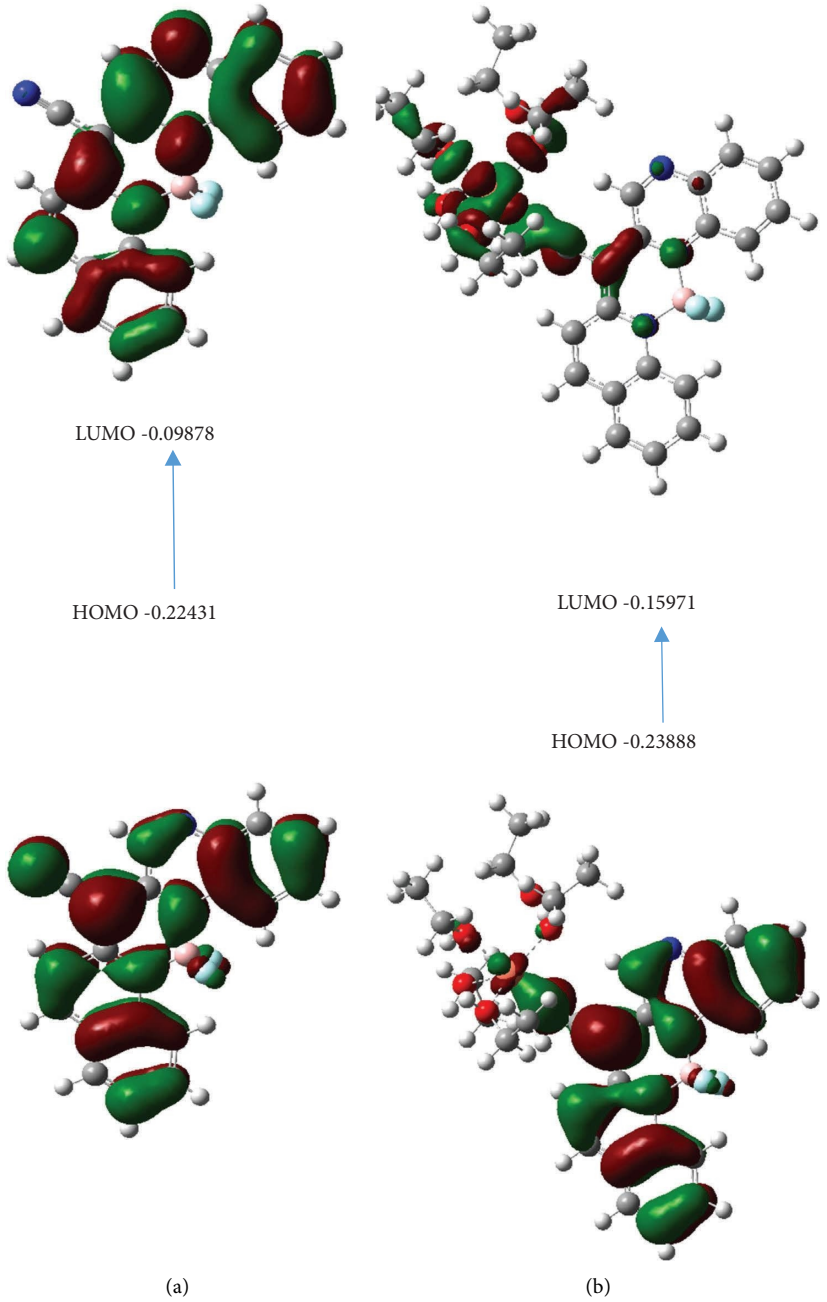

Figure 13: Frontier orbitals and their energies for (a) ligand calculated in ethanol and (b) Cu complex with ethanol molecules calculated in ethanol.

4. Conclusion

(1) The low photochemical quantum yield and high fluorescent quantum yield, together with the short-excited state lifetime value confirm that the studied dye is a highly recommended efficient laser dye.

(2) There is a correspondence between the measured results and the theoretically calculated results using the TD-DFT method.

(3) DBDMA dye in solutions undergoes energy transfer to fluorescein dye and fluorescence energy quenching by copper and cadmium ions.

(4) The studied dye is not considered an effective sensor for identifying the types of solvents or determining the medium's acidity.

Data Availability

The data used to support the findings of this study are available from the corresponding author upon request.

Disclosure

Samples of the compound are available from the authors.

Conflicts of Interest

The authors declare that there are no conflicts of interest.

Acknowledgments

The authors extend their appreciation to the Deputyship for Research & Innovation, Ministry of Education, Saudi Arabia, for funding this research work through the project number (QU-IF-4-5-3-29972). The authors also thank Qassim University for its technical support.

Supplementary Materials

The file of the supplementary material contains absorption and fluorescence spectra of the DBDMA dye in different solvents (Figures 1S and 2S), normalized spectra of the dye that show the mirror image relationships between absorption and fluorescence (Figure 3S), and absorption and excitation (Figure 4S). Figure 5S shows the fluorescence spectra using different excitation wavelengths. Figure 6S shows fluorescence decay of the profile, and Figure 7S shows the emission spectra in the presence of oxygen in the dye solution. Figure 8S presents the graphical representation of the energy transfer process modeled by the Stern–Volmer equation in the absence and the presence of $CuSO_4$ additive, respectively. Tables 1S and 2S present the coordinates of Cu^{+2}-DBDMA complex. (*Supplementary Materials*)

References

[1] N. Boens, V. Leen, and W. Dehaen, "Fluorescent indicators based on BODIPY," *Chemical Society Reviews*, vol. 41, no. 3, pp. 1130–1172, 2012.

[2] S. Erbas, A. Gorgulu, M. Kocakusakogullari, and E. U. Akkaya, "Non-covalent functionalized SWNTs as delivery agents for novel Bodipy-based potential PDT sensitizers," *Chemical Communications*, vol. 33, pp. 4956–4958, 2009.

[3] R. Ziessel, G. Ulrich, and A. Harriman, "The chemistry of Bodipy: a new El Dorado for fluorescence tools," *New Journal of Chemistry*, vol. 31, no. 4, pp. 496–501, 2007.

[4] P. A. Bouit, K. Kamada, P. Feneyrou et al., "Two-photon absorption-related properties of functionalized BODIPY dyes in the infrared range up to telecommunication wavelengths," *Advances in Materials*, vol. 21, no. 10-11, pp. 1151–1154, 2009.

[5] S. Kolemen, Y. Cakmak, S. Erten-Ela et al., "Solid-state dye-sensitized solar cells using red and near-IR absorbing bodipy sensitizers," *Organic Letters*, vol. 12, no. 17, pp. 3812–3815, 2010.

[6] M. Hesari, J. S. Lu, S. N. Wang, and Z. F. Ding, "Efficient electrochemiluminescence of a boron-dipyrromethene (BODIPY) dye," *Chemical Communications*, vol. 51, no. 6, pp. 1081–1084, 2015.

[7] A. Kamkaew, S. H. Lim, H. B. Lee, L. V. Kiew, L. Y. Chung, and K. Burgess, "BODIPY dyes in photodynamic therapy," *Chemical Society Reviews*, vol. 42, no. 1, pp. 77–88, 2013.

[8] D. Wang, R. Liu, C. Chen et al., "Synthesis, photophysical and electrochemical properties of aza-boron-diquinomethene complexes," *Dyes and Pigments*, vol. 99, no. 1, pp. 240–249, 2013.

[9] A. Poirel, A. De Nicola, and R. Ziessel, "Oligothienyl-BODIPYs: red and near-infrared emitters," *Organic Letters*, vol. 14, no. 22, pp. 5696–5699, 2012.

[10] Y. Hayashi, N. Obata, M. Tamaru et al., "Facile synthesis of biphenyl-fused BODIPY and its property," *Organic Letters*, vol. 14, no. 3, pp. 866–869, 2012.

[11] J. Huang, J. Su, and H. Tian, "The development of anthracene derivatives for organic light-emitting diodes," *Journal of Materials Chemistry*, vol. 22, pp. 10977–10989, 2012.

[12] G. Sathyamoorthi, M. L. Soong, T. W. Ross, and J. H. Boyer, "Fluorescent tricyclic β-azavinamidine–BF2 complexes," *Heteroatom Chemistry*, vol. 4, no. 6, pp. 603–608, 1993.

[13] E. Ahmed, T. Earmme, and S. A. Jenekhe, "New solution-processable electron transport materials for highly efficient blue phosphorescent OLEDs," *Advances in Functional Materials*, vol. 21, no. 20, pp. 3889–3899, 2011.

[14] J. Bañuelos, F. L. Arbeloa, V. Martinez et al., "Difluoro-boron-triaza-anthracene: a laser dye in the blue region. Theoretical simulation of alternative difluoro-boron-diaza-aromatic systems," *Physical Chemistry Chemical Physics*, vol. 13, no. 8, pp. 3437–3445, 2011.

[15] M. E. Kondakova, J. C. Deaton, T. D. Pawlik et al., "Highly efficient fluorescent-phosphorescent triplet-harvesting hybrid organic light-emitting diodes," *Journal of Applied Physics*, vol. 107, no. 1, Article ID 014515, 2010.

[16] E. Krystkowiak, "Effect of solute–solvent hydrogen-bonding on spectral and photophysical properties of aromatic probes," in *Hydrogen-Bonding Research in Photochemistry, Photobiology, and Optoelectronic Materials*, pp. 1–27, World Scientific, Singapore, 2019

[17] S. M. Al-Hazmy, Y. El-Ghoul, J. Al-Harby, H. Tar, and F. M. Alminderej, "Synthesis, characterization, and performance of Pyridomethene–BF_2 fluorescence dye-doped PVA thin film and PVP nanofibers as low γ-ray dosimeters," *ACS Omega*, vol. 7, no. 38, pp. 34002–34011, 2022.

[18] J. Al-Harby, H. Tar, and S. M. Al-Hazmy, "Photoinduced and classical sol-gel synthesis: spectral and photophysical behavior of silica matrix doped by novel fluorescent dye based on boron difluoride complex," *Polymers*, vol. 13, no. 16, p. 2743, 2021.

[19] S. A. El-Daly, S. M. Al-Hazmy, E. M. Ebeid et al., "Spectral, acid-base, and laser characteristics of 1,4-Bis[β-(2-quinolyl) vinyl]benzene (BQVB)," *Journal of Physical Chemistry*, vol. 100, no. 23, pp. 9732–9737, 1996.

[20] B. J. Coe, J. A. Harris, I. Asselberghs et al., "Quadratic nonlinear optical properties of N-aryl stilbazolium dyes," *Advances in Functional Materials*, vol. 12, no. 2, pp. 110–116, 2002.

[21] A. Mnasri, A. Mejri, S. M. Al-Hazmy et al., "Silver–N-heterocyclic carbene complexes-catalyzed multicomponent reactions: synthesis, spectroscopic characterization, density functional theory calculations, and antibacterial study," *Archiv der Pharmazie*, vol. 354, no. 9, Article ID 2100111, 2021.

[22] A. D. Becke, "A new mixing of Hartree-Fock and local density-functional theories," *The Journal of Chemical Physics*, vol. 98, no. 2, pp. 1372–1377, 1993.

[23] Y. Yang, M. N. Weaver, and K. M. Merz, "Assessment of the "6-31+G** + LANL2DZ" mixed basis set coupled with density functional theory methods and the effective core potential: prediction of heats of formation and ionization potentials for first-row-transition-metal complexes," *Journal of Physical Chemistry A*, vol. 113, no. 36, pp. 9843–9851, 2009.

[24] A. Szukalski, P. Krawczyk, B. Sahraoui, F. Rosińska, and B. Jędrzejewska, "A modified oxazolone dye dedicated to

spectroscopy and optoelectronics," *Journal of Organic Chemistry*, vol. 87, no. 11, pp. 7319–7332, 2022.

[25] D. P. Herten, A. Haderspeck, F. Braun, and H. Wadepohl, "Copper(II)-induced fluorescence quenching of a BODIPY fluorophore," *Zeitschrift für Anorganische und Allgemeine Chemie*, vol. 644, no. 14, pp. 735–739, 2018.

[26] C. H. Zhao, E. Sakuda, A. Wakamiya, and S. Yamaguchi, "Highly emissive diborylphenylene-containing bis(phenylethynyl)benzenes: structure–photophysical property correlations and fluoride ion sensing," *Chemistry - A European Journal*, vol. 15, no. 40, pp. 10603–10612, 2009.

[27] S. A. El-Daly, S. M. Al-Hazmy, E. M. Ebeid, and E. M. Vernigor, "Emission characteristics and photostability of 1, 4-bis [β-(2-benzoxazolyl) vinyl] benzene (BBVB) laser dye," *Journal of Photochemistry and Photobiology A: Chemistry*, vol. 91, no. 3, pp. 199–204, 1995.

[28] C. V. Bindhu, S. S. Harilal, V. P. N. Nampoori, and C. P. G. Vallabhan, "Solvent effect on absolute fluorescence quantum yield of Rhodamine 6G determined using transient thermal lens technique," *Modern Physics Letters B*, vol. 13, no. 16, pp. 563–576, 1999.

[29] E. M Ebeid and S. M. Al-Hazmy, *Photophysical and Laser Based Techniques in Chemistry, Biology and Medicine*, BookSurge Publishing, Charleston, SC, USA, 2006.

[30] P. Bhavya, R. Melavanki, M. N. Manjunatha, V. Koppal, N. R. Patil, and V. T. Muttannavar, "Solvent effects on the photophysical properties of coumarin dye," *AIP Conference Proceedings*, vol. 1953, Article ID 080022, 2018.

[31] P. S. Kadolkar, S. A. Patil, M. Y. Kariduraganavar, and S. R. Inamdar, "Evaluation of ground and excited state dipole moments of alexa fluor 350-NHS ester in binary mixtures of DMSO-water," *AIP Conference Proceedings*, vol. 2104, Article ID 030029, 2019.

[32] A. N. Al-romaizan and M. A. Hussein, "A new candidate laser dye based 1,4-Bis[β-(2-Naphthothiazolyle)Vinyl]Benzene. Spectroscopic behavior, laser parameters and excitation energy transfer," *Journal of Fluorescence*, vol. 28, no. 3, pp. 743–758, 2018.

[33] A. A. AboAlhasan, M. A. S. Sakr, M. F. Abdelbar et al., "Enhanced energy transfer from diolefinic laser dyes to meso-tetrakis (4-sulfonatophenyl) porphyrin immobilized on silver nanoparticles: DFT, TD-DFT and spectroscopic studies," *Journal of Saudi Chemical Society*, vol. 26, no. 4, Article ID 101491, 2022.

[34] N. L. Lavrik and N. U. Mulloev, "A method to study polydispersity of humic acid from fluorescence quenching by Cu^{2+} ions," *Journal of Applied Spectroscopy*, vol. 78, no. 5, pp. 705–710, 2011.

[35] M. H. Gehlen, "The centenary of the Stern-Volmer equation of fluorescence quenching: from the single line plot to the SV quenching map," *Journal of Photochemistry and Photobiology C: Photochemistry Reviews*, vol. 42, Article ID 100338, 2020.